ELSEVIER

Applied Clay Science 15 (1999) 11–29

APPLIED CLAY SCIENCE

Polymer-layered silicate nanocomposites: an overview

Peter C. LeBaron, Zhen Wang, Thomas J. Pinnavaia *

Department of Chemistry, Center for Fundamental Materials Research and Composite Materials and Structure Center, Michigan State University, East Lansing, MI 48824, USA

Received 12 December 1998; accepted 12 April 1999

Abstract

An overview of polymer–clay hybrid nanocomposites is provided with emphasis placed on the use of alkylammonium exchanged smectite clays as the reinforcement phase in selected polymer matrices. A few weight percent loading of organoclay in nylon 6 boosts the heat distortion temperature by 80°C, making possible structural applications under conditions where the pristine polymer would normally fail. A similar loading of clay nanolayers in elastomeric epoxy and polyurethane matrices dramatically improves both the toughness and the tensile properties of these thermoset systems. Glassy epoxy nanocomposites exhibit substantial improvement in yield strength and modulus under compressive stress–strain conditions. The latest development in polypropylene hybrids have yielded nanocomposites with improved storage moduli. Polyimide hybrids in thin-film form display a 10-fold decrease in permeability toward water vapor at 2 wt.% clay loading. In situ and melt intercalation processing methods are effective in producing reinforced polystyrene hybrids. Nitrile rubber hybrids show improved storage moduli and reduced permeabilities even toward gases as small as hydrogen. Poly(ε-caprolactone)–clay nanocomposites prepared by in situ polymerization of ε-caprolactone in organoclay galleries show a substantial reduction in water adsorption. Polysiloxane nanocomposites produced from poly(dimethylsiloxane) and organoclay mixtures have improved in tensile properties, thermal stability and resistance to swelling solvents. Organoclay-poly(*l*-lactide) composite film was obtained by solvent casting technique. Clay nanolayers dispersed in liquid crystals act as structure directors and form hybrids composites that can be switched from being highly opaque to highly transparent by applying an electric field of short duration. © 1999 Published by Elsevier Science B.V.

Keywords: polymers; silicates; nanocomposites

* Corresponding author. Fax: +1-517-432-1225; E-mail: pinnavai@cem.msu.edu

0169-1317/99/$ - see front matter © 1999 Published by Elsevier Science B.V.
PII: S0169-1317(99)00017-4

1. Introduction

Composites that exhibit a change in composition and structure over a nanometer length scale have been shown over the last 10 years to afford remarkable property enhancements relative to conventionally-scaled composites (Schmidt, 1985; Novak, 1993; Mark, 1996). Layered silicates dispersed as a reinforcing phase in an engineering polymer matrix are one of the most important forms of such ''hybrid organic–inorganic nanocomposites'' (Okada and Usuki, 1995; Giannelis, 1996; Ogawa and Kuroda, 1997). Although the high aspect ratio of silicate nanolayers is ideal for reinforcement, the nanolayers are not easily dispersed in most polymers due to their preferred face-to-face stacking in agglomerated tactoids. Dispersion of the tactoids into discrete monolayers is further hindered by the intrinsic incompatibility of hydrophilic layered silicates and hydrophobic engineering plastics. However, as was first demonstrated by the Toyota group more than 10 years ago (Fukushima and Inagaki, 1987), the replacement of the inorganic exchange cations in the galleries of the native clay by alkylammonium surfactants can compatibilize the surface chemistry of the clay and the hydrophobic polymer matrix. ε-Caprolactam was polymerized in the interlayer gallery region of the organoclay to form a true nylon 6–clay nanocomposite (Usuki et al., 1993a,b). At a loading of only 4.2 wt.% clay, the modulus doubled, the strength increased more than 50%, and the heat distortion temperature increased by 80°C compared to the pristine polymer (see Table 1). They also demonstrated that organoclays exfoliated in a nylon 6 polymer matrix greatly improved the dimensional stability, the barrier properties and even the flame retardant properties (Kojima et al., 1993a,b; Gilman et al., 1997). More significantly, these composites have been in use in under-the-hood applications in the automobile industry (Okada and Usuki, 1995).

The use of organoclays as precursors to nanocomposite formation has been extended into various polymer systems including epoxys, polyurethanes, polyimides, nitrile rubber, polyesters, polypropylene, polystyrene and polysiloxanes, among others. For true nanocomposites, the clay nanolayers must be uniformly

Table 1
Mechanical and thermal properties of nylon 6–clay composites (Kojima et al., 1993a,b,c)

Composite type	wt.% Clay	Tensile strength (MPa)	Tensile modulus (GPa)	Impact (kJ/m^2)	HDT (°C) at 18.5 kg/cm^2
''Nanoscopic'' (exfoliated)	4.2	107	2.1	2.8	145
''Micro'' (tactoids)	5.0	61	1.0	2.2	89
Pristine polymer	0	69	1.1	2.3	65

dispersed (exfoliated) in the polymer matrix, as opposed to being aggregated as tactoids or simply intercalated (see Fig. 1). Once nanolayer exfoliation has been achieved, the improvement in properties can be manifested as an increase in tensile properties, as well as enhanced barrier properties, decreased solvent uptake, increased thermal stability and flame retardance (Okada and Usuki, 1995; Giannelis, 1996).

The complete dispersion of clay nanolayers in a polymer optimizes the number of available reinforcing elements for carrying an applied load and deflecting cracks. The coupling between the tremendous surface area of the clay ($\sim 760\ m^2/g$) and the polymer matrix, facilitates stress transfer to the reinforcement phase, allowing for such tensile and toughening improvements. Conventional polymer–clay composites containing aggregated nanolayer tactoids ordinarily improve rigidity, but they often sacrifice strength, elongation and toughness. However, exfoliated clay nanocomposites, such as those that have been achieved for nylon 6 and epoxy systems, have to the contrary shown improvements in all aspects of their mechanical performance. High aspect ratio nanolayers also provide properties that are not possible for larger-scaled composites. The impermeable clay layers mandate a tortuous pathway for a permeant to transverse the nanocomposite (Fig. 2). The enhanced barrier characteristics, chemical resistance, reduced solvent uptake and flame retardance of clay–poly-

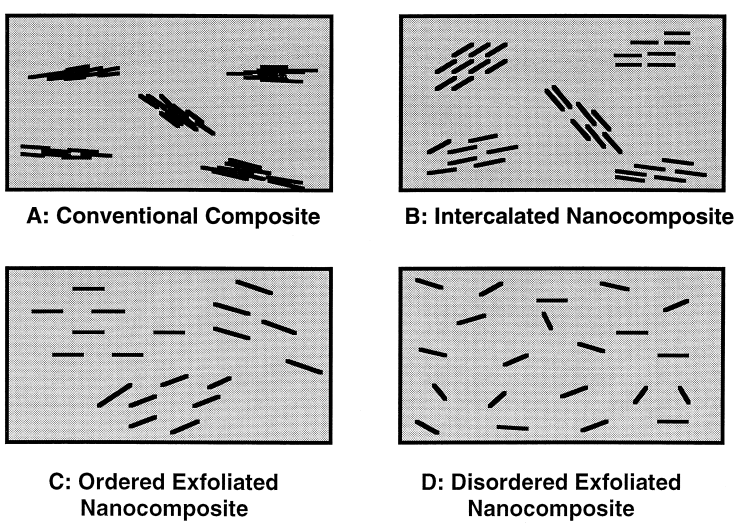

Fig. 1. Schematic illustrations of (A) a conventional; (B) an intercalated; (C) an ordered exfoliated; and (D) a disordered exfoliated polymer–clay nanocomposite. The clay interlayer spacing is fixed in an intercalated nanocomposite. On the other hand, in an exfoliated nanocomposite, the average gallery height is determined by clay silicate loading. The difference between ordered and disordered exfoliated nanocomposites is that the former can be detected by X-ray diffraction and the latter is X-ray amorphous.

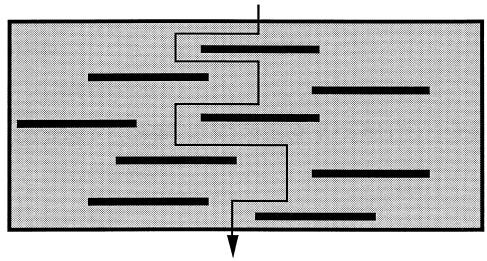

Fig. 2. Proposed model for the torturous zigzag diffusion path in an exfoliated polymer–clay nanocomposite when used as a gas barrier (Yano et al., 1993).

mer nanocomposites all benefit from the hindered diffusion pathways through the nanocomposite.

2. Organoclay structures and modeling

The replacement of inorganic exchange cations by organic onium ions on the gallery surfaces of smectite clays not only serves to match the clay surface polarity with the polarity of the polymer, but it also expands the clay galleries. This facilitates the penetration of the gallery space (intercalation) by either the polymer precursors or preformed polymer. Depending on the charge density of clay and the onium ion surfactant, different arrangements of the onium ions are possible. In general, the longer the surfactant chain length, and the higher the charge density of the clay, the further apart the clay layers will be forced. This is expected since both of these parameters contribute to increasing the volume occupied by the intragallery surfactant. Depending on the charge density of the clay, the onium ions may lie parallel to the clay surface as a monolayer, a lateral bilayer, a pseudo-trimolecular layer, or an inclined paraffin structure as illustrated in Fig. 3. At very high charge densities, large surfactant ions can adopt lipid bilayer orientations in the clay galleries.

The orientations of onium ion chains in organoclay were initially deduced based on infrared and XRD measurements (Lagaly, 1986). More recent modeling experiments has provided further insights into the packing orientations of the alkyl chains in organically modified layered silicates (Hackett et al., 1998). Molecular dynamics (MD) simulations were used to study molecular properties such as density profiles, normal forces, chain configurations and trans-gauche conformer ratios. For the mono-, bi- and psuedo-trilayers with respective *d*-spacings of 13.2, 18.0 and 22.7 Å, a disordered liquid-like arrangement of chains was preferred in the gallery. In this disordered arrangement the chains do not remain flat, but instead, overlap and co-mingle with onium ions in opposing layers within the galleries. However, for the trilayer arrangement, the methylene groups are primarily found within a span of two layers and only occasionally do

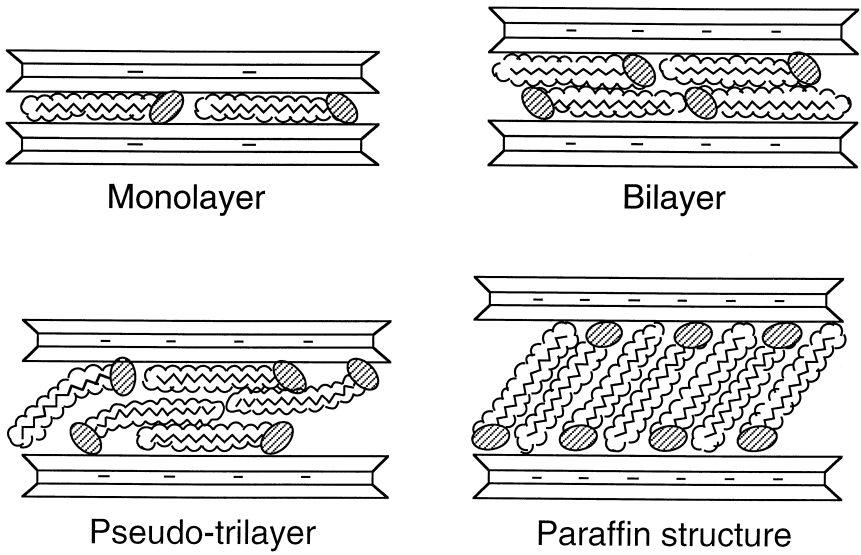

Fig. 3. Orientations of alkylammonium ions in the galleries of layered silicates with different layer charge densities (Lagaly, 1986).

they continue into the layer opposite to the positive head group. As anticipated, the onium head group is also noted to reside nearer the silicate surface relative to the aliphatic portion of the surfactant. The highest preference conformer is

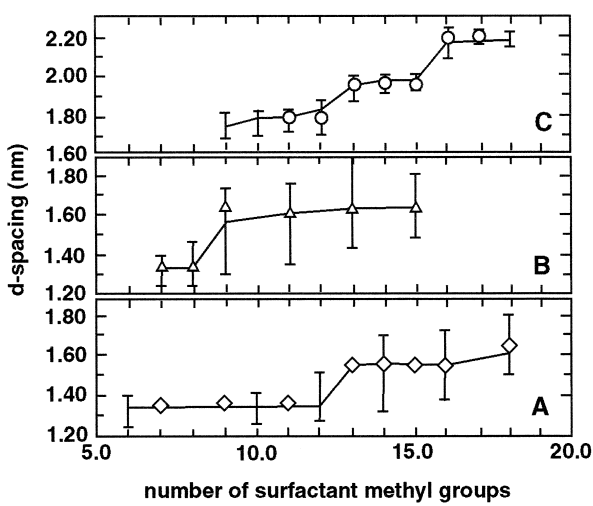

Fig. 4. Experimental (vertical bars) and simulated (symbols) values of the *d*-spacings for alkylammonium exchanged layered silicates at three different cation exchange capacities (CEC): (A) SWy2 montmorillonite, CEC = 0.8 meq/g; (B) AMS montmorillonite (Nanocor), CEC = 1.0 meq/g; (C) fluorohectorite (Dow-Corning), CEC = 1.5 meq/g. (Hackett et al., 1998).

trans over gauche for the maximum surfactant chain length just before the system progresses to the next highest layering pattern. This is expected since the alkyl chains must be optimally packed under such dense surfactant concentrations. The internal gallery pressure determines the *d*-spacing of an organoclay, which is shown in Fig. 4 for three different clays with varying surfactant length. The MD simulation experiments have agreed well with experimental XRD data and FTIR spectroscopy for the stacked intragallery alkyl chains, however, the inclined paraffin association (experimentally seen for $> C_{15}$ surfactants with clays of CEC = 1.2 meq/g and greater) is not addressed and would be a prime target for future modelings.

3. Organoclay–polymer interactions

If the polarity of the organoclay sufficiently matches the monomer or prepolymer, it will intercalate into the galleries, further spreading clay layers apart. Examples of such behavior have been observed for ε-caprolactam (Usuki et al., 1993a), epoxides (Lan and Pinnavaia, 1995) and polyols (Wang and Pinnavaia, 1998a) that intercalate organoclay galleries as unreacted precursors. For long chain onium-exchanged organoclays, the galleries swollen by these precursors show a *d*-spacing indicative of a paraffin monolayer arrangement (Fig. 5). Even these ideally matched systems, however, do not necessarily form true nanocomposites. Only when the clay layers are forced apart and no longer interact through the onium chains is an ideal nanocomposite formed upon polymerization (see Fig. 1C and D). The complete dispersal, or exfoliation, of the clay nanolayers yields composites with the highest degree of property enhancement. If the layers persist with a repeating layer stacking pattern with the gallery height less than two times the onium ion chain length, then the final product is said to be an intercalated composite which will have regions of very high and very low reinforcer concentration (Fig. 1B). This non-uniform disper-

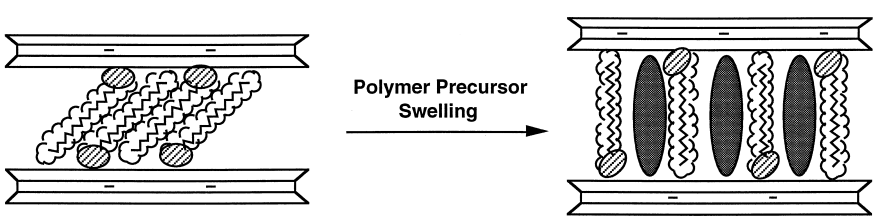

Fig. 5. Proposed model for the swelling of alkylammonium exchanged clay with a paraffin structure by polymer precursors such as ε-caprolactam, epoxide and polyol. However, regardless of the initial charge density of the clay and the orientations of the gallery long chain alkylammonium ions, the gallery height is determined by the vertical orientation of the long chain alkylammonium in the solvated intercalates. Cross-hatched ellipses represent the intercalated polymer precursor species.

sal of nanolayers limits stress transfer throughout the composite, giving comparatively less than optimal reinforcement. Still poorer, conventionally scaled composites are possible if the clay and polymer exhibit only partial miscibility (Fig. 1A). Here, the clay persists as tactoids of face-to-face stacked agglomerates throughout the polymer matrix. This incomplete dispersal of the reinforcing phase inhibits ideal surface contact between the polymer and clay, creating large regions of pure polymer in the composite.

Therefore, it is imperative that the surface polarities of polymer and clay be matched in order for the polymer to fully wet and intercalate clay tactoids. The aforementioned nylon 6 and epoxy–clay systems have achieved this exfoliated state and yielded nanocomposites with remarkable properties. Another important feature of these two systems is that protonated alkyl amine cations can catalyze the intragallery polymerization process. This speeds the congested intragallery reaction relative to the bulk polymer, providing a driving force for nanolayer exfoliation in the final composite. Other polymer–clay systems have since been studied with varying degrees of success, as summarized below.

4. Nanocomposite synthesis, characterization and properties

4.1. Epoxy–clay nanocomposites

Clay nanolayers have been shown to be very effective reinforcements in epoxy systems (Lan and Pinnavaia, 1994; Messersmith and Giannelis, 1994; Massam and Pinnavaia, 1998). The key to achieving an exfoliated epoxy–clay nanocomposite structure is first to load the clay gallery with hydrophobic onium ions, and then expand the gallery region by diffusing in the epoxide, the curing agent or a mixture of the two. Interestingly, acidic onium ions catalyze intragallery polymerization at a rate that is competitive with extragallery polymerization. However, the relative rates of reagent intercalation, chain formation and network cross-linking have to be controlled in order to form the gel state and, eventually, the fully cured epoxy-exfoliated clay nanocomposite (Wang and Pinnavaia, 1998b). Aliphatic amine, aromatic amine, anhydride and catalytic curing agents all have been chosen to form an epoxy matrix with broad glass transition temperatures. However, the clay nanolayers are more effective in improving mechanical properties when the polymer is in its rubbery state vs. the glassy state. For instance, 7.5 vol.% of the exfoliated 10 Å-thick silicate layers improves the strength of elastomeric polymer matrix by more than 10-fold (Lan and Pinnavaia, 1994). More recent work has also shown that clay nanolayers reinforce glassy epoxy matrices under compressive strain (Fig. 6). The dimensional stability, thermal stability and solvent resistance of the glassy matrix can also be improved when the clay nanolayers are present (Massam and Pinnavaia, 1998).

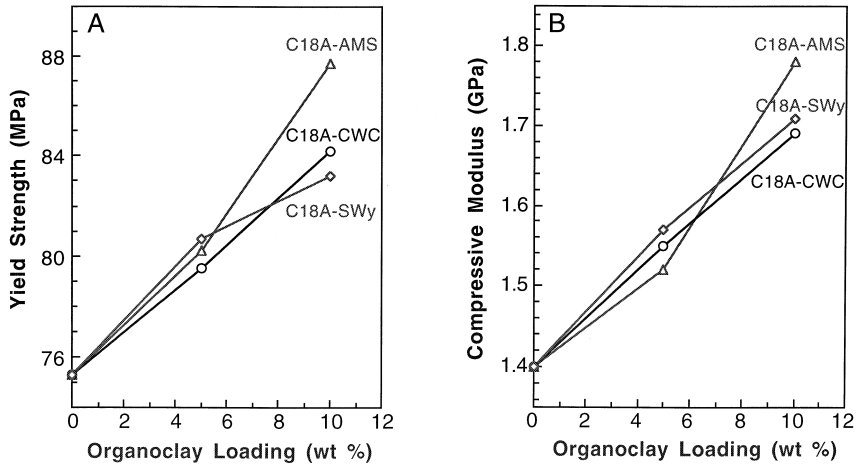

Fig. 6. Compressive (A) yield strength and (B) moduli for the pristine epoxy polymer and the exfoliated epoxy–clay nanocomposites prepared from three different kinds of organomontmorillonites. The epoxide resin and curing agent used in this system are EPON 826 and JEFFAMINE D-230, respectively (Massam and Pinnavaia, 1998).

4.2. Polyurethane–clay nanocomposites

The intercalation and exfoliation chemistry of epoxy–clay nanocomposites have been successfully transferred to a thermoset polyurethane system. The maximum benefit from nanolayer dispersal and reinforcement was demonstrated recently by Wang and Pinnavaia (1998a). Solvation of the organoclays by polyols afforded intercalates with basal spacings that were dependent on the chain length of the gallery onium ion, but independent of the molecular weight of the polyol or the cation exchange capacity of the clay. In situ polymerization of polyol–isocyanate precursor–organoclay mixtures afforded nanocomposites containing an intercalated clay phase (~ 50 Å basal spacings) embedded in the cross-linked polyurethane network. A unique stress–strain behavior was observed for the elastomeric nanocomposites (Fig. 7). Nanocomposite formation both strengthens and toughens the elastomeric matrix relative to the pristine polymer.

4.3. Polypropylene–clay hybrids

The dispersal of clay nanolayers into the nonpolar polyolefin systems proves to be a challenge since the polarity of organoclay does not match well with such polymers. Initial attempts to create polypropylene–clay hybrids were based on the introduction a modified polypropylene with polar groups to mediate the polarity between the clay surface and bulk polypropylene (Kurokawa et al., 1996; Usuki et al., 1997). However, an organic solvent has to be used in order to

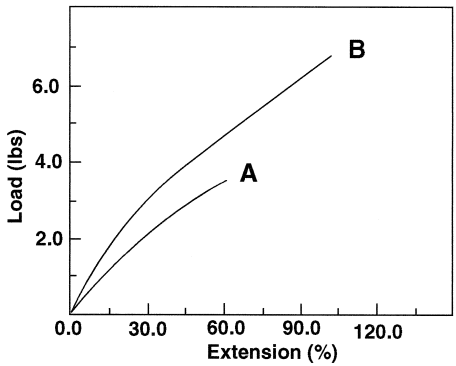

Fig. 7. Stress–strain curves for (A) a pristine polyurethane elastomer; (B) a polyurethane–clay nanocomposite prepared from organomontmorillonite (5 wt.%) (Wang and Pinnavaia, 1998a).

facilitate the formation of a modified polypropylene intercalate. Only a limited degree of clay nanolayer dispersion was observed by this method. An alternative and more environmentally friendly approach was developed later by the Toyota research group (Kawasumi et al., 1997; Kato et al., 1997; Hasegawa et al., 1998). The mixture of stearylammonium-exchanged montmorillonite, maleic anhydride modified polypropylene oligomer and homopolypropylene was melt-processed to obtain a successful polypropylene–clay hybrid wherein a larger fraction of the clay nanolayers were found to be exfoliated. The hydrolyzed maleic anhydride polypropylene intercalated into the organoclay, expanding the galleries, and facilitated the incorporation of polypropylene. Interestingly, the density of maleic anhydride groups has a significant effect on the final morphology and properties of the composite. A mixture of roughly 3:1 by mass of maleic anhydride polypropylene oligomer to organoclay was found to be the most effective in forming hybrid composites. The hybrids exhibit improved storage moduli compared to pristine polypropylene in the temperature range from T_g to 90°C. The significance of nanolayer reinforcement in polypropylene is not as great as in nylon 6, probably due to the lower degree of exfoliation and the introduction of a large amount of oligomer. However, polypropylene–clay nanocomposites are still attractive for applications as packaging materials where enhanced barrier properties are desired.

4.4. Polyimide–clay hybrids

The benefit of polymer–clay nanocomposite formation was successfully demonstrated in the polyimide system by showing dramatically improved barrier properties and a heightened thermal stability. Polyimide–clay nanocomposite films are produced from the polymerization of 4,4′-diaminodiphenyl ether and pyromellitic dianhydride in dimethylacetamide (DMAC) solvent as outlined in

Fig. 8 (Yano et al., 1993). For reasons not well known, synthetic mica and montmorillonite were found to yield largely exfoliated hybrids, while saponite and hectorite retain a monolayer of intercalation (Yano et al., 1997). A separate study showed that a large fraction of montmorillonite nanolayers is in the aggregated form rather than the exfoliated form (Lan et al., 1994). Nevertheless, regardless of the degree of dispersal of clay layers, mass transport studies of polyimide–clay nanocomposites revealed a several-fold reduction in the permeability of small gases, e.g., O_2, H_2O, He, CO_2, and the organic vapor ethyl acetate with the presence of only small fraction of organoclay. For instance, at 2 wt.% clay loading, the permeability coefficient of water vapor was decreased ten fold for the synthetic mica relative to pristine polyimide (Yano et al., 1997). By comparing hybrids made with clays of various aspect ratios not only was the permeability noted to decrease with increasing aspect ratio (Fig. 9), but also the thermal expansion coefficient decreased for an identical loading with increasing nanolayer aspect ratio (hectorite 50, saponite 170, montmorillonite 220, synthetic mica 1230).

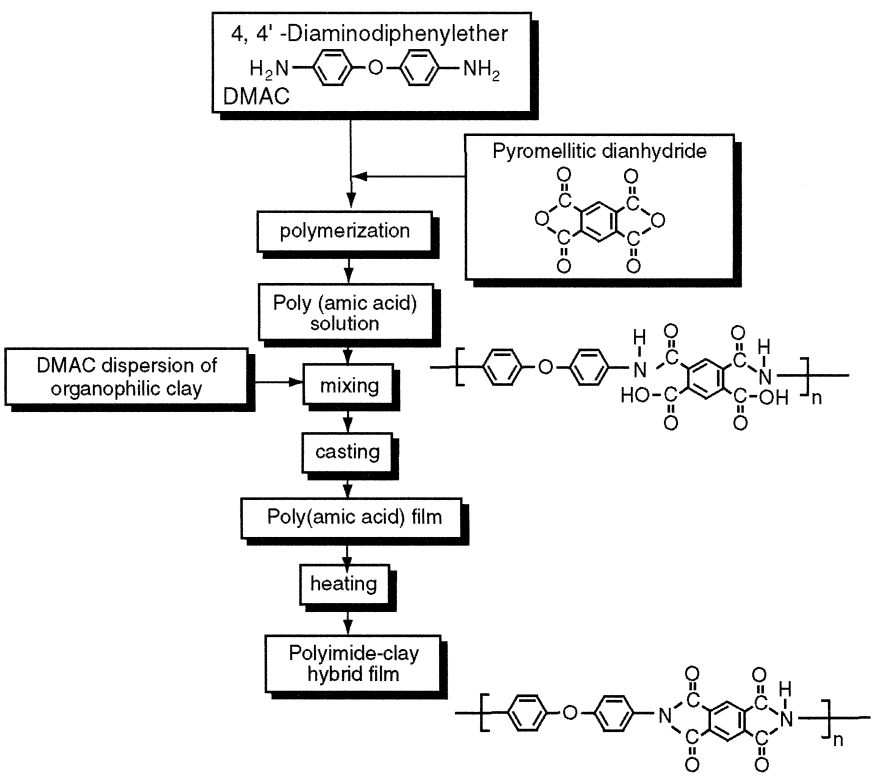

Fig. 8. Synthesis of polyimide–clay hybrid film (Yano et al., 1997).

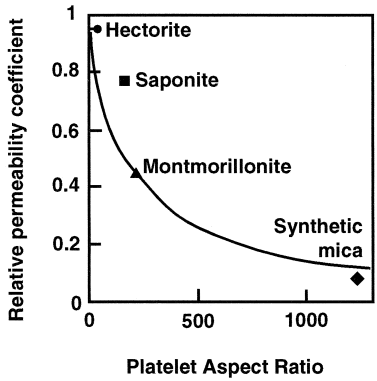

Fig. 9. The reduction of the relative permeability coefficient is dependent on the clay platelet aspect ratio in the system of polyimide–clay hybrid with water vapor as the permeate. Each hybrid contains 2 wt.% clay. The aspect ratios for hectorite, saponite, montmorillonite and synthetic mica are 46, 165, 218 and 1230, respectively (Yano et al., 1997).

4.5. Polystyrene–clay nanocomposites

Different techniques have been employed in order to form polystyrene nanocomposites. One method used a Cu^{2+} exchanged hectorite instead of the more common organoclay (Porter et al., 1998). The copper cations were expected to catalyze the oxidation of styrene monomers in the clay galleries, but the approach was unsuccessful, most likely due to the inability of styrene to intercalate into the inorganic clay. An alternative technique involved the direct bonding of styrene to a vinyl functionalized surfactant exchanged into the organoclay via in situ polymerization (Akelah and Moet, 1996). Still, there must first be a gallery expansion invoked by the addition an organic solvent in order for the styrene to intercalate prior to polymerization. Acetonitrile proved to be the most effective solvent as it gave a 24.5 Å *d*-spacing indicating intercalation of styrene (vs. 22.2 and 18.1 Å for acetonitrile–THF and acetonitrile–toulene mixtures, respectively). Following polymerization the XRD peak for the intercalated clay persisted, indicating that little or no exfoliation of the clay occurred.

The most practical and promising technique for polystyrene intercalation was the melt intercalation of the polymer into the interlayer gallery region of the clay. Both long chain primary and quaternary alkylammonium exchanged clays were examined (Vaia et al., 1995, 1996; Vaia and Giannelis, 1997). The organoclay was mixed with commercially available polystyrene at a temperature above T_g of the polymer via melt processing. The diffusion of the polystyrene polymer into the intragallery region was a slow process, dependent on many factors such as the polymer molecular weight, processing temperature, alkylammonium chain length and the interactions between the polymer, surfactant and silicate. Under optimal processing conditions, about 10 Å thickness of polymer

was inserted into clay gallery with a very limited fraction of disordered silicate layers presented near the edge of crystallites.

4.6. Rubber–clay hybrids (RCHs)

A Na^+ exchanged form of montmorillonite was ion-exchanged with a protonated form of butadiene and acrylonitrile copolymer (ATBN) with a functionalized amino end group (MW = 3400) in the presence of co-solvents water and *N,N*-dimethyl sulphoxide (Kojima et al., 1993c). The final composite was obtained by mixing the ATBN intercalated clay with nitrile rubber under cross-linking (vulcanizing) conditions. The TEM micrograph of the RCH showed that the silicate nanolayers were highly dispersed in the rubber matrix. The permeabilities of hydrogen and water vapor for the RCH were reduced by about one third relative to the pristine nitrile rubber. A separate study also showed that the rubber–clay nanocomposite significantly reduced the permeability of oxygen. The potential applications for these nanocomposites include tire inner-liners and inner-tubes (Kresge and Lohse, 1996).

Poly(styrene-*b*-butadiene) copolymer–clay nanocomposites also have been prepared from dioctadecyldimethyl ammonium exchanged montmorillonite using a similar approach (Laus et al., 1997). The composite samples were prepared by mixing the organoclay with copolymer pellets at 120°C, and annealing at 120°C for an additional 16–73 h. While the identical mixing of copolymer with a Na^+ unexchanged montmorillonite showed no intercalation, the organoclay expanded from 41 to 46 Å, indicating a monolayer intercalation. The final nanocomposites showed an increasing storage modulus (Fig. 10) with increasing

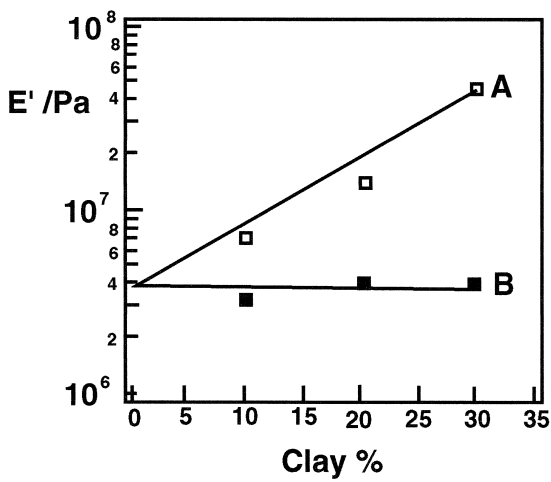

Fig. 10. The storage modulus E' at 25°C for (A) poly(styrene-*b*-butadiene)–clay nanocomposites prepared from dioctadecyldimethyl ammonium-exchanged montmorillonite and (B) conventional composites prepared from Na^+-montmorillonite (Laus et al., 1997).

loading. Also, the T_g for the polystyrene block domain increased with clay content, whereas the polybutadiene block domain T_g remained nearly constant.

4.7. Poly(ε-caprolactone)–clay nanocomposites

An earlier effort to prepare poly(ε-caprolactone)–clay nanocomposites by in situ polymerization of ε-caprolactone in Cr^{3+}-fluorohectorite was not successful (Messersmith and Giannelis, 1993). Only a very limited degree of intercalation of the poly(ε-caprolactone) polymer into the hydrophilic clay galleries was observed, meaning the catalytic properties of Cr^{3+} went unutilized. When the inorganic cations were replaced by the protonated 12-aminododecanoic acid, followed by the in situ polymerization of ε-caprolactone at 170°C, a higher degree of silicate nanolayer dispersion in the polymer matrix was achieved (Messersmith and Giannelis, 1995). The X-ray analysis of the final nanocomposite lacked low-angle reflections, indicating that the layers have been delaminated in the polycaprolactone matrix. The 12-aminolauric acid not only made the intragallery swellable at elevated temperatures, but it also catalyzed the intragallery polymerization. The poly(ε-caprolactone)–clay nanocomposite film was prepared by a casting technique. The nanocomposite barrier properties were studied by monitoring the adsorption of H_2O through the nanocomposite film into a desiccant. At 4.8% silicate by volume the film showed a five fold reduction in permeability compared to the pure polymer as shown in Fig. 11. As demonstrated previously for the nylon 6 and polyimide systems, the permeant molecules must transverse a tortuous path due to the presence of silicate nanolayers in the polymer matrix.

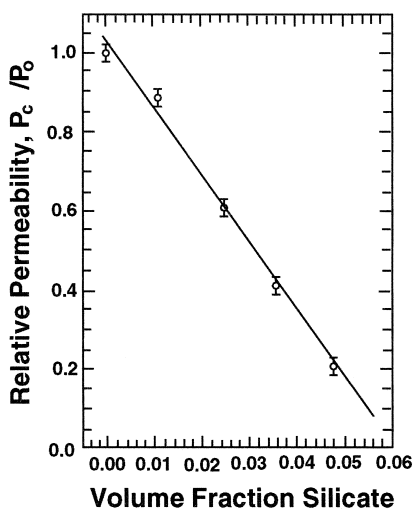

Fig. 11. Relative permeability (P_c / P_o) vs. volume fraction of clay for poly(ε-caprolactone)–montmorillonite nanocomposites (Messersmith and Giannelis, 1995).

4.8. Polysiloxane–clay nanocomposites

Polysiloxane elastomers have been reported to be reinforced by precipitated silica particles which are nanosized and highly dispersed through a sol–gel technique (Mark, 1996). Organoclay nanotechnology has provided an alternative approach to preparing silicate-reinforced polysiloxane nanocomposites. Dimethylditallow ammonium exchanged montmorillonite, where tallow is a mixture of C_{18}, C_{16}, C_{14} and C_{12} alkyl chains, was combined with an 18,000 molecular weight silanol terminated poly(dimethylsiloxane) (PDMS), and then cross-linked with tetraethylorthosilicate (TEOS) in the presence of tin octoate as catalyst (Burnside and Giannelis, 1995). Interestingly, small additions of H_2O were needed in order achieve exfoliated nanocomposites (Fig. 12).

Exchanging Na^+ montmorillonite with other organic surfactants such as benzyldimethyloctadecylammonium prohibited intercalation by PDMS prepolymers as only the original organoclay peak persisted. In contrast, the exfoliated nanocomposite obtained with dimethylditallow ammonium clay showed somewhat increased thermal stability, noted by TGA as the 10% clay loading exhibited a delayed decomposition. The nanocomposite also showed a much reduced solvent uptake relative to other PDMS composites where the filler was kaolin or carbon black.

A separate PDMS–clay study made comparisons between the tensile properties of aerosilica–PDMS hybrids and clay–PDMS hybrids made from both the direct addition of organoclay and PDMS (melt intercalation), and organoclay dispersed in chloroform (solution intercalation) (Wang et al., 1998). While the melt intercalated pure organoclay did not achieve as high a reinforcement as the

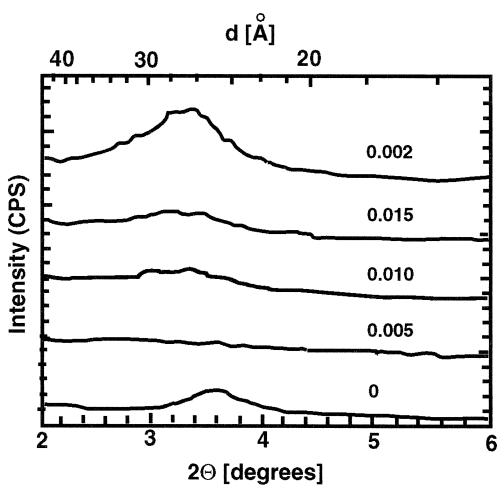

Fig. 12. X-ray diffraction patterns of poly(dimethylsiloxane)–clay nanocomposites prepared from dimethyl ditallowammonium exchanged montmorillonite as a function of the weight ratio of water to silicate (Burnside and Giannelis, 1995).

aerosilica–silicone hybrid, the clay nanocomposite formed from solution had a nearly identical reinforcing affect on tensile strength as the aerosilica composite.

4.9. Organoclay–polymer blends

Water soluble polymers have been found to be miscible with inorganic clay in aqueous suspension (Theng, 1979). More recently, the blending of organoclay with preformed thermoplastic polymers in an organic solvent has been examined. For instance, poly(*l*-lactide) (PLLA) pellets were mixed with distearyldimethylammonium-exchanged organomontmorillonite and blended together in hot chloroform. After the chloroform was fully vaporized, 100 μm thick films remained. PLLA did not intercalate into the organoclay and tactoids of pure clay were detected parallel to the surface of the films. The clay platelets further aligned themselves to the film surface as the films were drawn out (Ogata et al., 1997a). While the PLLA–clay system demonstrated an example of a solvent-cast organophillic polymer–clay blend, the absence of clay delamination gave relatively poor tensile improvements compared to true nanocomposites. Other organic solvent-cast composites included a poly(ethyleneoxide)–clay blend and a poly(ε-caprolactone)–clay blend (Jimenez et al., 1997; Ogata et al., 1997b).

4.10. Liquid crystal–clay hybrids

Other recent advancements in polymer–clay nanocomposites have included organoclay–liquid crystal nanocomposites that show a unique light scattering effect controlled by electric field, temperature change or shearing. Na^+-montmorillonite was ion-exchanged with 4-(4′-cyanobiphenyl-4-oxy) butyl ammonium (CBAM) (Kawasumi et al., 1996a) or 4-cyano(4′-biphenyloxy) undecyl ammonium (CBUM) (Kawasumi et al., 1996b) to obtain organoclays that can be homogeneously dispersed in nematic crystal matrices. The liquid crystal phases are 4-pentyl-4′-cyanobiphenyl (5CB) and nematic TFALC (TFALC is a mixture of low molar mass liquid crystals) for the CBAM and CBUM organoclay, respectively.

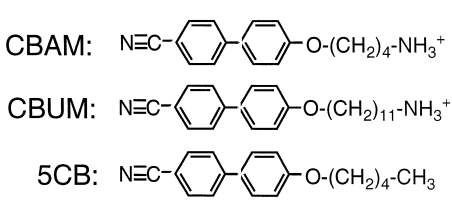

Initially, a cell of the liquid crystalline composite (LCC) containing the above organoclay scattered light strongly. However, upon the application of a low

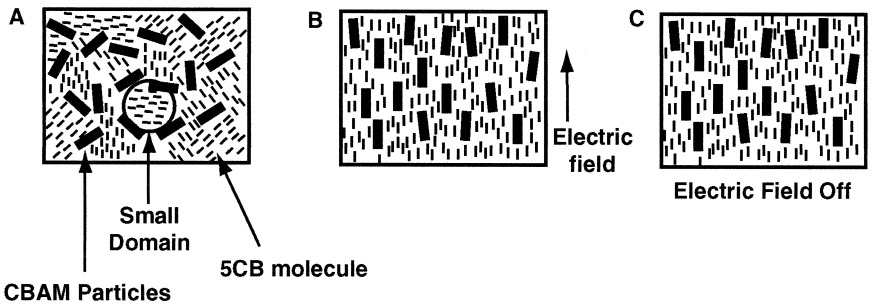

Fig. 13. A schematic illustration of the mechanism for the electro-optic effect of liquid crystalline composites prepared from organoclay. (A) the initial state of LCC; (B) when an electric field is applied to LCC; (C) the memory state of LCC is maintained after the electric field is switched off (Kawasumi et al., 1996b).

frequency electrical field, the cell became transparent. The liquid crystal showed a strong dielectric anisotropy, becoming aligned parallel to the electric field. This forced a similar alignment of the clay which minimized scattering and increased transparency. The clay layers then appeared to act as anchors, as they prohibited the reformation of a random matrix, leading to a semi-transparent memory state which remained for months after the electric field was turned off (Fig. 13). More recent liquid crystal work has indicated that the application of a high frequency field can erase the memory state and return the nanocomposite to the original opaque state wherein the clay is randomly dispersed. Future applications could include adjustable light-controlling glass, erasable optical storage devices and thermo-optical sensors.

5. Conclusions

Organically modified smectite clays can be effective reinforcing agents in the synthesis of polymer–clay nanocomposites. By inserting long chain surfactants into the hydrophilic galleries of the native clay, the interlayer distance increases, and the surface chemistry of the clay is modified. In an ideal system, these newly rendered organophilic galleries allow for the intercalation of monomer or prepolymer, and eventually the formation of exfoliated nanocomposites. The surfactant exchange cations, particularly when protonated, can also serve to catalyze intragallery polymerization reactions. This facilitates the delamination of clay in the polymer matrix by biasing the intragallery reaction relative to the bulk polymer and thus forces the clay to disperse into distinct nanolayers. Although surfactant cations mediate the clay–polymer interaction, and in some cases speed the intragallery polymerization, one possible drawback due to the presence of monofunctional cations is that they can compromise nanocomposite properties (Wang and Pinnavaia, 1998b). For thermoset polymers, the insertion

of the onium ion functional group onto the polymer chain can form terminal ends that block the cross-linking of the polymer. This plasticizing effect resulting from dangling chains located at the clay interface can be especially detrimental at high clay loadings.

Efforts to create true nanocomposites with new polymer systems will encounter the unavoidable obstacle of adequately matching the surface polarity of the clay and the polymer. This must be accomplished in order to allow the polymer to intercalate into the galleries in route to forming the final nanocomposite. The addition of solvents, and more recently, the implication of a third oligomeric phase, are currently being examined as reagents to compatibilize the relatively short chain surfactants in the organoclay and the high molecular weight polymer being reinforced. The melt processing of mixtures of organoclay, oligomer (compatabilizer) and preformed polymer in hydrophobic thermoplastic polymer systems seems to be very promising for nanocomposite formation.

Future research will address these and other issues facing the design of polymer–clay nanocomposites. The polymer–clay systems that have been studied this far provided a basis for refinement, and further work will furnish valuable insight into the mechanisms of reinforcement and new methods of nanocomposite design.

Acknowledgements

The support of the MSU Center for Fundamental Materials Research and the Composite Materials and Structure Center is gratefully acknowledged.

References

Akelah, A., Moet, A., 1996. Polymer–clay nanocomposites: free-radical grafting of polystyrene on to organophilic montmorillonite interlayers. J. Mater. Sci. 31, 3589–3596.

Burnside, S.D., Giannelis, E.P., 1995. Synthesis and properties of new poly(dimethylsiloxane) nanocomposites. Chem. Mater. 7, 1597–1600.

Fukushima, Y., Inagaki, S., 1987. Synthesis of an intercalated compound of montmorillonite and 6-polyamide. J. Inclusion Phenom. 5, 473–482.

Giannelis, E.P., 1996. Polymer layered silicate nanocomposites. Adv. Mater. 8, 29–35.

Gilman, J.W., Kashiwagi, T., Lichtenhan, J.D., 1997. Nanocomposites: a revolutionary new flame retardant approach. SAMPE J. 33, 40–46.

Hackett, E., Manias, E., Giannelis, E.P., 1998. Molecular dynamics simulations of organically modified layered silicates. J. Chem. Phys. 108, 7410–7415.

Hasegawa, N., Kawasumi, M., Kato, M., Usuki, A., Okada, A., 1998. Preparation and mechanical properties of polypropylene–clay hybrids using a maleic anhydride-modified polypropylene oligomer. J. Appl. Polym. Sci. 67, 87–92.

Jimenez, G., Ogata, N., Kawai, H., Ogihara, T., 1997. Structure and thermal/mechanical properties of poly(ε-caprolactone)–clay blend. J. Appl. Polym. Sci. 64, 2211–2220.

Kato, M., Usuki, A., Okada, A., 1997. Synthesis of polypropylene oligomer–clay interaction compounds. J. Appl. Polym. Sci. 63, 1781–1785.

Kawasumi, M., Hasegawa, N., Usuki, A., Okada, A., 1996a. Novel memory effect found in nematic liquid crystal/fine particle system. Liq. Cryst. 21, 769–776.

Kawasumi, M., Usuki, A., Okada, A., Kurauchi, T., 1996b. Liquid crystalline composite based on a clay mineral. Mol. Cryst. Liq. Cryst. 281, 91–103.

Kawasumi, M., Hasegawa, N., Kato, M., Usuki, A., Okada, A., 1997. Preparation and mechanical properties of polypropylene–clay hybrids. Macromolecules 30, 6333–6338.

Kojima, Y., Usuki, A., Kawasumi, M., Okada, A., Fukushima, Y., Kurauchi, T., Kamigaito, O., 1993a. Mechanical properties of nylon 6–clay hybrid. J. Mater. Res. 8, 1185–1189.

Kojima, Y., Usuki, A., Kawasumi, M., Okada, A., Kurauchi, T., Kamigaito, O., 1993b. Sorption of water in nylon 6–clay hybrid. J. Appl. Polym. Sci. 49, 1259–1264.

Kojima, Y., Fukumori, K., Usuki, A., Okada, A., Kurauchi, T., 1993c. Gas permeabilities in rubber–clay hybrid. J. Mater. Sci. Lett. 12, 889–890.

Kresge, E.N., Lohse, D.J., 1996. Composite tire innerliners and inner tubs. US Patent 5,576,372.

Kurokawa, Y., Yasuda, H., Oya, A., 1996. Preparation of a nanocomposite of polypropylene and smectite. J. Mater. Sci. Lett. 15, 1481–1483.

Lagaly, G., 1986. Interaction of alkylamines with different types of layered compounds. Solid State Ionics 22, 43–51.

Lan, T., Pinnavaia, T.J., 1994. Clay-reinforced epoxy nanocomposites. Chem. Mater. 6, 2216–2219.

Lan, T., Pinnavaia, T.J., 1995. Mechanism of clay tactoid exfoliation in epoxy–clay nanocomposites. Chem. Mater. 7, 2144–2150.

Lan, T., Kaviratna, P.D., Pinnavaia, T.J., 1994. On the nature of polyimide–clay hybrid composites. Chem. Mater. 6, 573–575.

Laus, M., Francescangeli, O., Sandrolini, F., 1997. New hybrid nanocomposites based on an organophilic clay and poly(styrene-*b*-butadiene) copolymers. J. Mater. Res. 12, 3134–3139.

Mark, J.E., 1996. Ceramic-reinforced polymers and polymer-modified ceramics. Polym. Eng. Sci. 36, 2905–2920.

Massam, J., Pinnavaia, T.J., 1998. Clay nanolayer reinforcement of a glassy epoxy polymer. Mater. Res. Soc. Symp. Proc. 520, 223–232.

Messersmith, P.B., Giannelis, E.P., 1993. Polymer-layered silicate nanocomposites: in situ intercalative polymerization of ε-caprolactone in layered silicates. Chem. Mater. 5, 1064–1066.

Messersmith, P.B., Giannelis, E.P., 1994. Synthesis and characterization of layered silicate–epoxy nanocomposites. Chem. Mater. 6, 1719–1725.

Messersmith, P.B., Giannelis, E.P., 1995. Synthesis and barrier properties of poly(ε-caprolactone)-layered silicate nanocomposites. J. Polym. Sci., Part. A: Polym. Chem. 33, 1047–1057.

Novak, B.M., 1993. Hybrid nanocomposites materials between inorganic glasses and organic polymers. Adv. Mater. 5, 422–433.

Ogata, N., Jimenez, G., Kawai, H., Ogihara, T., 1997a. Structure and thermal/mechanical properties of poly(*l*-lactide)–clay blend. J. Polym. Sci., Part B: Polym. Phys. 35, 389–396.

Ogata, N., Kawakage, S., Ogihara, T., 1997b. Structure and thermal/mechanical properties of poly(ethylene oxide)–clay mineral blends. Polymer 38, 5115–5118.

Ogawa, M., Kuroda, K., 1997. Preparation of inorganic–organic nanocomposites through intercalation of organoammonium ions into layered silicates. Bull. Chem. Soc. Jpn. 70, 2593–2618.

Okada, A., Usuki, A., 1995. The chemistry of polymer–clay hybrids. Mater. Sci. Eng. C 3, 109.

Porter, T.L., Hagerman, M.E., Reynolds, B.P., Eastman, M.P., Parnell, R.A., 1998. Inorganic/organic host–guest materials: surface and interclay reactions of styrene with copper(II)-exchanged hectorite. J. Polym. Sci., Part B: Polym. Phys. 36, 673–679.

Schmidt, H., 1985. New type of non-crystalline solids between inorganic and organic materials. J. Non-Cryst. Solids 73, 681–691.

Theng, B.K.G., 1979. Formation and Properties of Clay–Polymer Complexes. Elsevier, New York.

Usuki, A., Kawasumi, M., Kojima, Y., Okada, A., 1993a. Swelling behavior of montmorillonite cation exchanged for ω-amino acids by ε-caprolactam. J. Mater. Res. 8, 1174–1178.

Usuki, A., Kojima, Y., Kawasumi, M., Okada, A., Fukushima, Y., Kurauchi, T., Kamigaito, O., 1993b. Synthesis of nylon 6-clay hybrid. J. Mater. Res. 8, 1179–1184.

Usuki, A., Kato, M., Okada, A., Kurauchi, T., 1997. Synthesis of polypropylene–clay hybrid. J. Appl. Polym. Sci. 63, 137–139.

Vaia, R.A., Giannelis, E.P., 1997. Polymer melt intercalation in organically-modified layered silicates: model predications and experiment. Macromolecules 30, 8000–8009.

Vaia, R.A., Jandt, K.D., Kramer, E.J., Giannelis, E.P., 1995. Kinetics of polymer melt intercalation. Macromolecules 28, 8080–8085.

Vaia, R.A., Jandt, K.D., Kramer, E.J., Giannelis, E.P., 1996. Microstructural evolution of melt intercalated polymer–organically modified layered silicates nanocomposites. Chem. Mater. 8, 2628–2635.

Wang, Z., Pinnavaia, T.J., 1998a. Nanolayer reinforcement of elastomeric polyurethane. Chem. Mater. 10, 3769–3771.

Wang, Z., Pinnavaia, T.J., 1998b. Hybrid organic–inorganic nanocomposites: exfoliation of magadiite nanolayers in an elastomeric epoxy polymer. Chem. Mater. 10, 1820–1826.

Wang, S., Li, Q., Qi, Z., 1998. Studies on silicone rubber/montmorillonite hybrid composites. Key Eng. Mater. 137, 87–93.

Yano, K., Usuki, A., Okada, A., Kurauchi, T., Kamigaito, O., 1993. Synthesis a properties of polyimide–clay hybrid. J. Polym. Sci., Part A: Polym. Chem. 31, 2493–2498.

Yano, K., Usuki, A., Okada, A., 1997. Synthesis and properties of polyimide–clay hybrid films. J. Polym. Sci., Part A: Polym. Chem. 35, 2289–2294.